

1 **Thiostrepton hijacks pyoverdine receptors to inhibit growth of *Pseudomonas aeruginosa***

2 Michael R. Ranieri, Derek C. K. Chan, Luke Yaeger, Madeleine Rudolph, Sawyer Karabelas-Pittman,
3 Hamdi Abdo, Jessica Chee, Hanjeong Harvey, Uyen Nguyen, and Lori L. Burrows.

4 Department of Biochemistry and Biomedical Sciences, and the Michael G. DeGroote Institute for
5 Infectious Diseases Research, McMaster University, Hamilton, ON

6

7 **Running title:** Thiostrepton inhibits growth of *Pseudomonas aeruginosa*

8

9 **Keywords:** antibiotic, thiopeptide, iron, siderophore, gram negative

10

11 ***Correspondence to:**

12 Dr. Lori L. Burrows

13 4H18 Health Sciences Centre, 1280 Main St. West,

14 Hamilton, ON L8S 4K1 Canada

15 Tel: 905-525-9140 x 22029 Fax: 905-522-9033 Email: burrowl@mcmaster.ca

16

17 **ABSTRACT**

18 *Pseudomonas aeruginosa* is a biofilm-forming opportunistic pathogen and intrinsically resistant to many
19 antibiotics. In a high-throughput screen for molecules that modulate biofilm formation, we discovered
20 that the thiopeptide antibiotic, thiostrepton (TS) - considered inactive against Gram-negative
21 bacteria - stimulated *P. aeruginosa* biofilm formation in a dose-dependent manner. This phenotype is
22 characteristic of exposure to antimicrobial compounds at sub-inhibitory concentrations, suggesting that
23 TS was active against *P. aeruginosa*. Supporting this observation, TS inhibited growth of a panel of 96
24 multidrug-resistant (MDR) *P. aeruginosa* clinical isolates at low micromolar concentrations. TS also had
25 activity against *Acinetobacter baumannii* clinical isolates. Expression of Tsr - a 23S rRNA-modifying
26 methyltransferase - in trans conferred TS resistance, confirming that the drug acted via its canonical
27 mode of action, inhibition of ribosome function. Deletion of oligopeptide permease systems used by
28 other peptide antibiotics for uptake failed confer TS resistance. TS susceptibility was inversely
29 proportional to iron availability, suggesting that TS exploits uptake pathways whose expression is
30 increased under iron starvation. Consistent with this finding, TS activity against *P. aeruginosa* and *A.*
31 *baumannii* was potentiated by FDA-approved iron chelators deferiprone and deferasirox. Screening of *P.*
32 *aeruginosa* mutants for TS resistance revealed that it exploits pyoverdine receptors FpvA and FpvB to
33 cross the outer membrane. Our data show that the biofilm stimulation phenotype can reveal cryptic
34 sub-inhibitory antibiotic activity, and that TS has activity against select multidrug resistant Gram-
35 negative pathogens under iron-limited growth conditions, similar to those encountered at sites of
36 infection.

37 **INTRODUCTION**

38 Bacterial pathogens are rapidly evolving resistance to available antibiotics, creating an urgent need
39 for new therapies. Gram-negative bacteria are particularly challenging to treat because their outer
40 membranes limit the access of many drugs to intracellular targets (1). Resistance arises when bacteria
41 accumulate target mutations, acquire specific resistance determinants, increase drug efflux, and/or
42 enter antibiotic-tolerant dormant or biofilm modes of growth (2). Biofilms consist of surface-associated
43 bacteria surrounded by self-produced extracellular polymeric substances (EPS). Biofilm architecture
44 allows for development of phenotypic heterogeneity that leads to variations in susceptibility as well as
45 the formation of drug-tolerant persister cells (3). Approaches with the potential to preserve current
46 antibiotics include combining them with biofilm inhibitors, resistance blockers (e.g. ampicillin with

47 clavulanic acid or piperacillin with tazobactam), efflux inhibitors (e.g. PA β N), outer membrane
48 permeabilizers, or coupling them to molecules such as siderophores that are actively imported, so-called
49 Trojan horses (4).

50 Among the bacterial pathogens deemed most problematic by the World Health Organization is the
51 Gram-negative opportunist, *Pseudomonas aeruginosa* (5). It infects immunocompromised patients –
52 particularly those with medical devices – and is a major problem for people with severe burns or cystic
53 fibrosis (6). It is intrinsically resistant to many antibiotics and readily forms biofilms, further enhancing
54 its ability to evade therapy (7). The low permeability of its outer membrane and expression of multiple
55 efflux pumps that extrude a wide variety of substrates, coupled with its propensity to form biofilms,
56 limits the repertoire of effective anti-*Pseudomonas* antibiotics (8-10). Here with the initial aim of
57 identifying potential modulators of *P. aeruginosa* biofilm formation, we screened a collection of
58 bioactive molecules including previously FDA-approved off-patent drugs. During this work, we identified
59 several molecules that stimulated biofilm formation beyond our arbitrary cutoff of 200% of the vehicle
60 control. Investigation of one such stimulatory compound, thioestrepton (TS), revealed that it had low
61 micromolar activity against *P. aeruginosa* in minimal medium. Through a series of investigations, we
62 showed that TS gains access to its ribosomal targets by exploiting iron limitation-dependent uptake
63 pathways. These data show that the biofilm stimulation phenotype can reveal cryptic antibiotic activity
64 when concentrations are too low (or growth conditions not conducive) to inhibit growth.

65 RESULTS

66 Thioestrepton stimulates *P. aeruginosa* biofilm formation

67 We used a previously described *P. aeruginosa* biofilm assay (11) to screen a bespoke collection
68 of 3921 bioactive molecules that includes ~1100 FDA-approved, off-patent drugs and antibiotics (12).
69 The molecules were screened in duplicate at 10 μ M in a dilute growth medium consisting of 10%
70 lysogeny broth (LB), 90% phosphate buffered saline (henceforth, 10:90) to identify molecules capable of
71 modulating biofilm formation. This medium was chosen to minimize the amount of biofilm formed in
72 the presence of the vehicle control, so that molecules that stimulated biofilm formation could be more
73 easily identified. The hits were divided into planktonic growth inhibitors (60 compounds), biofilm
74 inhibitors (defined as those resulting in \leq 50% of vehicle control biofilm, 8 compounds), or biofilm
75 stimulators (those resulting in \geq 200% of vehicle-treated control biofilm, 60 compounds) (**Supplementary**
76 **Table S1**). The hit rate of ~3% was relatively high for a primary screen, but all the molecules in this

77 curated collection have biological activity. The hits belonged to a variety of chemical classes and
78 included drugs with nominally eukaryotic targets.

79 Multiple studies showed that sub-inhibitory concentrations of antibiotics from a variety of
80 classes and with different mechanisms of action (MOA) stimulate *P. aeruginosa* biofilm formation,
81 although the specific pathways underlying this response remain unclear (13-18). Among the molecules
82 in our screen that stimulated biofilm formation was the thiopeptide antibiotic, thiostrepton (TS; **Fig 1A**).
83 This response intrigued us because TS is considered ineffective against Gram-negative bacteria due to
84 the impermeability of the outer membrane (OM) to large hydrophobic compounds (19, 20). In dose-
85 response experiments in 10:90 medium, biofilm levels increased while planktonic cell density decreased
86 with increasing TS concentrations to 10 μ M (17 μ g/ml), the maximum that could be tested due to its
87 limited solubility (**Fig 1B**).

88 **Growth in minimal media increases susceptibility of *P. aeruginosa* to TS**

89 Environmental conditions can modulate the expression or essentiality of antibiotic targets or
90 alter the availability of particular nutrients (21), leading to changes in susceptibility. We hypothesized
91 that the biofilm response of *P. aeruginosa* to TS may be the result of nutrient deficiency in 10:90, which
92 was more limiting to *P. aeruginosa* growth than M9 minimal medium (**Supplementary Fig S1**). Growth in
93 Vogel Bonner Minimal Media (VBMM) in the absence of TS was similar to that in 10:90 (**Supplementary**
94 **Fig S1**) but in the presence of TS, planktonic cell density decreased to below the level of detection at
95 concentrations above \sim 1.25 μ M (**Fig 1C**). These data suggested that nutrient limitation enhances
96 susceptibility of *P. aeruginosa* to TS.

97 **The ribosomal methyltransferase *Tsr* protects *P. aeruginosa* against TS**

98 The established MOA for TS is inhibition of protein translation through direct binding to
99 bacterial ribosomes (22). However, because TS also has anti-parasitic and anti-neoplastic activities (23,
100 24) we considered the possibility that it might inhibit *P. aeruginosa* growth in a novel way. To validate
101 the MOA, we expressed a resistance gene, *tsr*, from a plasmid in *P. aeruginosa* strains PAO1 and PA14.
102 *tsr* encodes a 23s rRNA methyltransferase, used by TS producer *Streptomyces azureus* to prevent self-
103 intoxication (25). *Tsr* methylates the conserved A1067 residue of 23s rRNA, impairing binding of TS to its
104 target (26). Expression of *tsr* in trans increased TS resistance of both PAO1 and PA14 compared to
105 vector-only controls (**Fig 2**). PAO1 was resistant up to the maximum soluble TS concentration of 10 μ M,
106 while resistance of PA14 was significantly increased compared to control, although not to the same

107 extent as PAO1. These results suggest that TS inhibits growth via its canonical MOA of ribosome binding,
108 implying that it can cross the *P. aeruginosa* OM to access the bacterial cytoplasm.

109 **TS susceptibility increases in the presence of iron chelators**

110 To understand the reason for increased TS susceptibility of *P. aeruginosa* in VBMM compared to
111 10:90, we considered the differences in nutrient availability between the two media types. The primary
112 carbon source in 10% LB is amino acids (27) while the carbon source in VBMM is citrate (28). Citrate can
113 chelate divalent cations including calcium and magnesium, which are important for OM integrity. We
114 hypothesized that this chelation effect may increase OM permeability. To stabilize the OM, we repeated
115 the dose response assay in VBMM supplemented with 100 mM MgCl₂ but saw no effect on susceptibility
116 (**Supplementary Fig S2A**). Since TS is a thiopeptide, we next hypothesized that amino acid limitation
117 during growth in VBMM may increase uptake of TS, leading to growth inhibition. To test this, we
118 supplemented VBMM with 0.1% casamino acids, but saw no change in TS susceptibility (**Supplementary**
119 **Fig 2B**). Further, simultaneous deletion of components of the Opp (Npp) peptide transport system,
120 exploited by other peptide antibiotics for entry (29, 30), and a homologous system, Spp, had no effect
121 on TS susceptibility (**Supplementary Fig S2C**).

122 We next considered that VBMM was more iron-limited than 10:90, which contains trace iron
123 from yeast extract and peptone. Under iron limitation, bacteria secrete siderophores into the
124 extracellular milieu to scavenge the metal. Specialized receptors then transport siderophore-iron
125 complexes back into the cell. Some antimicrobials, including sideromycins, pyocins, and bacteriocins, use
126 siderophore receptors to access intracellular targets (31-34), and we hypothesized that TS may use this
127 strategy. We compared *P. aeruginosa* PAO1 grown in 10:90 with increasing concentrations of TS alone
128 (**Fig 3A**) or with 0.1μM EDDHA, a membrane-impermeable iron chelator (35) (**Fig 3B**). Addition of EDDHA
129 shifted biofilm stimulation and growth inhibition to lower concentrations of TS compared to 10:90
130 alone. Supplementation of 10:90 plus 0.1μM EDDHA with 100μM FeCl₃ increased planktonic cell density
131 and reduced biofilm stimulation (**Fig 3C**). These data suggest that TS susceptibility is inversely
132 proportional to iron availability, and that TS may exploit siderophore receptors to cross the OM of *P.*
133 *aeruginosa*.

134 The poor solubility of TS has hampered its development as a therapeutic, but these data
135 suggested that its effective concentration could be reduced in the presence of iron chelators. We tested
136 the FDA-approved iron chelators deferiprone (DFP) and deferasirox (DSX) for potential synergy with TS.

137 Checkerboard assays revealed that while neither chelator had activity against *P. aeruginosa* on its own,
138 both potentiated TS activity (**Fig 3DE**) at concentrations well below those used to safely treat patients,
139 up to 28 mg/kg/day for DSX or 99 mg/kg/day for DFP (36).

140 **TS hijacks pyoverdine receptors FpvA and FpvB**

141 To identify the route of iron-limitation dependent TS entry into *P. aeruginosa*, we tested the
142 susceptibility of mutants from the ordered PA14 transposon library (37) that had insertions in genes
143 encoding known siderophore receptors, as well as mutants with insertions in uncharacterized OM
144 proteins with homology to siderophore receptors. In VBMM, most mutants had an IC₅₀ of 0.16 μM (0.26
145 μg/ml), similar to the parental strain (**Table 1**). In contrast, an *fpvA* mutant, encoding the type I
146 pyoverdine receptor, had an IC₅₀ of 3.5 μM. Growth inhibition was still observed at the highest TS
147 concentrations, indicating that the *fpvA* mutant remained partially susceptible. *P. aeruginosa* encodes
148 two type I pyoverdine receptors, FpvA and FpvB, with ~39% amino acid identity (71% similarity). The
149 *fpvB* mutant was also less susceptible to TS than the parent strain, with an IC₅₀ of 1 μM. Based on these
150 patterns of susceptibility, we speculated that TS may use both FpvA and FpvB, but that FpvA was the
151 preferred receptor. When we deleted *fpvA* in the *fpvB* background, the double mutant was more
152 resistant to TS than the single mutants, with an IC₅₀ of 6.3 μM (**Table 1**). Complementation of the *fpvAB*
153 mutant with *fpvB* on a plasmid restored TS susceptibility to levels similar to those of the single *fpvA*
154 mutant (**Table 1**). Together, these data suggest that TS exploits both pyoverdine receptors for entry.

155 **TS is active against multi-drug resistant clinical isolates**

156 To test whether TS could inhibit growth of a broader range of *P. aeruginosa* strains, particularly
157 multi-drug resistant (MDR) isolates for which there are fewer antibiotic options, we tested 96 recent
158 clinical isolates for susceptibility to TS in 10:90. While approximately 1 in 10 of those strains had an IC₅₀
159 ≥5μM TS (**Fig 4A**), a combination of 5 μM TS (8.3 μg/ml) plus 86 μM DSX (32 μg/ml) reduced growth of
160 all but three isolates of *P. aeruginosa* to less than 25% of the DMSO control (**Fig 4A**). We next tested the
161 activity of TS against another MDR Gram-negative pathogen that can cause severe infections,
162 *Acinetobacter baumannii* (38). *A. baumannii* strains encode FpvA and FpvB homologs (**Supplementary Fig**
163 **S3**), suggesting they may be susceptible to the thiopeptide. Growth of 6 of 10 *A. baumannii* strains in
164 10:90 was reduced to ≤50% of control with 5 μM TS, while the combination of 5μM TS and 86 μM DSX
165 reduced growth of 8/9 clinical isolates of *A. baumannii* below 10% of control (**Fig 4B**). As reported

166 previously (39), growth of *E. coli* – which lacks FpvAB homologs – was unaffected even at the maximum
167 soluble concentration of 10 μ M TS (not shown).

168 **DISCUSSION**

169 The natural role of antibiotics has been broadly debated (14, 16): are they signaling molecules
170 that are toxic at high concentrations, or weapons used by bacteria to gain an advantage over
171 competitors in their environment? The biofilm stimulation response to sub-inhibitory concentrations of
172 antibiotics is consistent with both views. At concentrations too low to elicit damage, bacteria show little
173 phenotypic response to antibiotic exposure. As concentrations approach the MIC, the bacteria respond
174 in a dose-dependent manner by ramping up the amount of biofilm produced – detecting either the
175 antibiotics or their effects – which may protect a subpopulation of cells. Above the MIC, antibiotics fall
176 into the deadly weapons category. Biofilm stimulation by sub-inhibitory concentrations of antibiotics is a
177 common phenomenon among multiple gram-positive and gram-negative species, and is caused by
178 several drug classes, suggesting it is not necessarily linked to a specific MOA (16, 18, 40). As
179 demonstrated here, this phenomenon can be used to identify potential antibiotic activity in the absence
180 of killing, a useful feature when screening at a single arbitrary concentration that may be below the MIC
181 for the drug-organism combination being tested. Interestingly, we and others (41) found that many
182 drugs intended for eukaryotic targets can impact bacterial growth and biofilm formation
183 (**Supplementary Table S1**), implying that they have deleterious effects on prokaryotic physiology. With a
184 new appreciation of the role of the human microbiome in health and disease, these potential effects
185 should be considered during drug development.

186 TS, a complex cyclic thiopeptide made by *Streptomyces azureus*, *S. hawaiiensis*, and *S. laurantii*,
187 is experiencing a resurgence of research interest due to its broad anti-bacterial, anti-malarial, and anti-
188 cancer activities (23, 24). It is a member of the RiPP (ribosomally synthesized and post-translationally
189 modified peptides) class of natural products (42), derived from a 42-amino acid precursor, TsrA (43).
190 Although the mechanism of its antibacterial activity (inhibition of translation by binding to helices
191 H43/H44 of 23S rRNA) and resistance (methylation of 23S rRNA residue A1067) have been deciphered
192 (26, 44), the way in which this ~1.7 kDa molecule enters target bacteria is unknown. Our data suggest
193 that TS is actively imported into *P. aeruginosa* under iron-restricted conditions.

194 There are multiple examples of molecules that exploit iron uptake pathways to enter bacteria.
195 Class I microcins – narrow-spectrum antibiotics produced by some gram negative species – bind to

196 siderophore receptors and share many of TS's properties. They are RiPPs, less than 5 kDa in mass, and
197 cyclic (giving them the nickname 'lasso peptides'). Notably, binding of iron by microcins is not a
198 prerequisite for uptake, as some interact with siderophore receptors in an iron-free state. For example,
199 MccJ25, produced by *E. coli* (45), interacts with siderophore receptor FhuA by mimicking the structure of
200 ferrichrome (46). It is not yet clear whether TS binds iron or simply mimics an iron-bound conformation,
201 as it has multiple hydroxyls positioned in a manner that could coordinate metals (**Fig 1A**). Its structure
202 has been solved both by X-ray crystallography and NMR, but no bound metals were reported (47, 48).
203 The FpvA receptor is also exploited by S-pyocins, 40-80 kDa peptide antibiotics produced by competing
204 *P. aeruginosa* strains, showing that it is a key promiscuous entry point for diverse molecules in addition
205 to its usual ligand, pyoverdine (33, 34, 49).

206 Our discovery that TS exploits FpvA and FpvB for uptake into the periplasm helps to explain the
207 resistance of gram-negative species such as *E. coli* to this antibiotic, as they lack those proteins.
208 Bioinformatic searches show FpvAB homologs are expressed by *P. aeruginosa* and related pathogens –
209 including *A. baumannii* (**Supplementary Fig S3**) – suggesting that TS could have utility as a narrow-
210 spectrum agent. Use of multiple pyoverdine receptors by TS may reduce the probability of resistance
211 arising through mutation of a single receptor, although genome analysis of clinical isolate C0379 that
212 was most resistant to the combination of TS and DSX (**Fig 4A**) revealed a wild type copy of *fpvA* coupled
213 with an ~800 bp deletion encompassing the 5' region of *fpvB*. Further investigation of *P. aeruginosa*
214 strains that are resistant to TS will be needed to understand the most likely routes by which it occurs.

215 Although TS uses siderophore receptors to cross the *P. aeruginosa* OM, the way in which this
216 large cyclic peptide transits the cytoplasmic membranes of gram-positive and gram-negative bacteria to
217 reach its ribosomal targets remains undefined. Expression of *tsr* in *P. aeruginosa* conferred resistance,
218 confirming that TS acts via its canonical bacteriostatic MOA. While PA14 expressing Tsr was significantly
219 more resistant to TS than the control, it was more sensitive than PAO1. This difference is not due to
220 nucleotide polymorphism at the Tsr methylation site on the rRNA, as these residues are conserved
221 between PAO1 and PA14. The reasons for strain-specific differences in susceptibility are unclear, but our
222 data confirm that most *P. aeruginosa* isolates tested (including MDR strains) are susceptible to TS,
223 especially when it is combined with DSX (**Fig 4A, Supplementary Table S2**).

224 TS's major liability is its poor solubility (50). Smaller, more soluble fragments that retain activity
225 against gram-positive bacteria and have reduced toxicity for eukaryotic cells have been identified (51)
226 but it is not clear if they would be active against *P. aeruginosa* if uptake by the FpvAB receptors requires

227 the intact molecule. Another way to circumvent solubility issues is to reduce the required concentration.
228 Our data show that this can be accomplished for TS by co-administration with FDA-approved iron
229 chelators DFP or DSX (**Fig 3DE**). The true potential of TS as an anti-infective may be underestimated, as
230 MIC evaluations are typically performed in rich, iron-replete media such as cation-adjusted Mueller-
231 Hinton broth. Many host environments are iron-restricted, particularly in the presence of infection and
232 inflammation (52-54) and future studies of TS activity should emulate those growth conditions.

233 In summary, we showed that biofilm stimulation can be used in high-throughput small molecule
234 screening to report on sub-inhibitory antibiotic activity that may otherwise be missed using the usual
235 metric of growth inhibition. In a small screen of less than 4000 molecules at a fixed concentration of 10
236 μM , we identified 60 molecules that stimulated biofilm formation, suggesting that they may have
237 antimicrobial activity at higher concentrations, or under different growth conditions, as demonstrated
238 here for TS. Stimulation of biofilm matrix production by TS in the gram-positive genus *Bacillus* was
239 reported previously, and that phenotype leveraged to identify novel thiopeptide producers in co-
240 cultures (55). Those studies, and the data presented here, suggest that monitoring biofilm stimulation
241 (or an easily assayed proxy thereof, such as increased expression from biofilm matrix promoters) could
242 allow for increased detection of molecules with potential antibacterial activity during screening, making
243 it a useful addition to the antimicrobial discovery toolkit.

244 **ACKNOWLEDGEMENTS**

245 We thank Gerry Wright for access to strains from the Wright Clinical Collection, David Heinrichs for
246 the gift of EDDHA and helpful discussions, and Neha Sharma, Andrew Hogan, Amanda Veri, and Victor
247 Yang for assistance with method development. This work was supported by a Natural Sciences and
248 Engineering Research (NSERC) grant RGPIN-2016-06521, and by Ontario Research Fund grant RE07-048.
249 MRR and UN held Ontario Graduate Scholarships, MR was supported by an NSERC Undergraduate
250 Summer Research Award, SKP was supported by a Summer Studentship from GlycoNet, and HA was
251 supported by a Summer Studentship from Cystic Fibrosis Canada.

252 **METHODS**

253 **Bacterial strains and culture conditions**

254 The bacterial strains and plasmids used in this study are listed in **Table 1** and **Supplementary Table**
255 **S2**. Bacterial cultures were grown in Lysogeny Broth (LB), 10:90 (10% LB and 90% phosphate buffered

256 saline), M9 medium, Vogel Bonner minimal medium (VBMM), or cation-adjusted Mueller-Hinton broth
257 (MBH) as indicated. Where solid media were used, plates were solidified with 1.5% agar. DFP (Sigma-
258 Aldrich) and DSX (Cayman Chemicals) were stored at 4°C until use. TS was stored at -20°C. A 60 mg/mL
259 stock solution of DFP was made in 6M HCl and Milli-Q H₂O (DFP solvent) in a ratio of 3:50. A 20 mg/mL
260 stock solution of DSX was made in DMSO. A 20mM stock solution of TS was made in DMSO.

261 **Growth curves**

262 PAO1-KP was inoculated from a -80°C stock into 5 ml LB broth and grown with shaking at 200 rpm,
263 16h, 37°C. The overnight culture was subcultured at 1:500 into 5 different media (LB, 10:90, M9,
264 Mueller-Hinton (MH), and VBMM) – incubated at 37°C for 6h with shaking at 200 rpm. Each subculture
265 was standardized to OD₆₀₀ ~ 0.1 (Biomate 3 Spectrophotometer) then diluted 1:500 into the same
266 medium. Six replicates of 200 µl of each sample were added to a 96 well plate, which was incubated at
267 37°C for 24 h with shaking at 200 rpm (Tecan Ultra Evolution plate reader). The OD₆₁₂ was read every 15
268 min for 24 h. The data for the six replicates of each sample were averaged and the experiment was
269 repeated 3 times. The final data with standard deviations were plotted using Prism (Graphpad).

270 **Biofilm modulation assay**

271 Biofilm formation was assayed as described in (11), with modifications. Briefly, *P. aeruginosa* was
272 inoculated in 5 mL of LB and grown at 37°C overnight, shaking at 200 rpm, and subsequently
273 standardized to an OD₆₀₀ of ~ 0.1 in 10:90. For the initial screen, 1 mM compound stocks in DMSO were
274 diluted 1:100 in standardized cell suspension (1.5 µL of compound stock in 148.5 µL of cell suspension)
275 to a final concentration of 10 µM. Control wells contained 10:90 plus 1% DMSO (sterility control) or
276 standardized cell suspension plus 1% DMSO (growth control). Biofilms were formed on polystyrene peg
277 lids (Nunc). After placement of the peg lid, the plate was sealed with parafilm to prevent evaporation
278 and incubated for 16 h at 37°C, 200 rpm. Following incubation, the 96-peg lid was removed and
279 planktonic density in the 96 well plate measured at OD₆₀₀ to assess the effect of test compounds on
280 bacterial growth. The lid was transferred to a new microtiter plate containing 200 µl of 1X phosphate-
281 buffered saline (PBS) per well for 10 min to wash off any loosely adherent bacterial cells, then to a
282 microtiter plate containing 200 µL of 0.1% (wt/vol) CV per well for 15 min. Following staining, the lid was
283 washed with 70 mL of dH₂O, in a single well tray, for 10 min. This step was repeated four times to ensure
284 complete removal of excess CV. The lid was transferred to a 96-well plate containing 200 µL of 33%
285 (vol/vol) acetic acid per well for 5 min to elute the bound CV. The absorbance of the eluted CV was

286 measured at 600 nm (BioTek ELx800), and the results plotted as percent of the DMSO control using
287 Prism (Graphpad). Screens were performed in duplicate. Compounds that resulted in <50% of control
288 biofilm were defined as biofilm inhibitors, while compounds that resulted in >200% of control biofilm
289 were defined as biofilm stimulators. Compounds of interest were further evaluated using the same
290 assay but over a wider range of concentrations (dose-response assay).

291 For TS dose response assays, TS stock solutions were diluted in DMSO and 2 μ L of the resulting
292 solutions plus 148 μ L of a bacterial suspension standardized to an OD₆₀₀ of ~ 0.1 in 10:90 were added to a
293 96 well plate in triplicate, as described above. Control wells contained 148 μ L of 10:90 + 1.3% DMSO
294 (sterility control) or standardized bacterial suspension + 1.3% DMSO (growth control). For EDDHA alone
295 or with FeCl₃ experiments, 2 μ L of each were added as aqueous solutions to reach final concentrations of
296 0.1 μ M EDDHA and 100 μ M FeCl₃, and the amount of bacterial suspension adjusted to keep the total well
297 volume at 150 μ L. Controls for EDDHA and FeCl₃ were 2 μ L of sterile dH₂O. Biofilms were grown for 16h at
298 37°C, 200 rpm, then stained and quantified as described above. Assays were performed in triplicate and
299 results were graphed using Prism (Graphpad) as a percentage of the DMSO control.

300 **Compounds screened**

301 The biofilm modulation assay was used to screen the McMaster Bioactives compound
302 collection. This curated collection includes off-patent, FDA-approved drugs from the Prestwick Chemical
303 Library (Prestwick Chemical, Illkirch, France), purified natural products from the Screen-Well Natural
304 Products Library (Enzo Life Sciences, Inc., Farmingdale, NY, USA), drug-like molecules from the
305 Lopac¹²⁸⁰ (International Version) collection (Sigma-Aldrich Canada Ltd., Oakville, ON, Canada) and the
306 Spectrum Collection (MicroSource Discovery Systems, Inc., Gaylordsville, CT, USA) which includes off
307 patent drugs, natural products, and other biologically active compounds. In total, the collection is 3921
308 unique compounds.

309 **Construction of a *tsr* plasmid for expression in *P. aeruginosa***

310 The *tsr* gene from pIJ6902 (56) was PCR-amplified using primers
311 5' GAATCCCGGGCGGTAGGACGACCATGAC 3' and 5' CTTC AAGCTTTTATCGGTTGGCCGCGAG 3'. Both the
312 PCR product and pUCP20 vector were digested with SmaI and HindIII, gel-purified, and ligated at a 1:3
313 molar ratio using T4 DNA ligase. The ligated DNA was transformed into *E. coli* DH5a and transformants
314 selected on LB agar containing 100 μ g/mL ampicillin and 5-bromo-4-chloro-3-indolyl- β -D-
315 galactopyranoside for blue-white selection. Plasmids from white colonies were purified using a GeneJet

316 Plasmid Miniprep kit (Thermo Scientific) following the manufacturer's protocols. After verification by
317 restriction digest and DNA sequencing, pUCP20 and pUCP20-tsr were each introduced into *P. aeruginosa*
318 PAO1 and PA14 by electroporation. Transformants were selected on LB agar containing 200 µg/mL
319 carbenicillin.

320 **IC₅₀ and checkboard assays**

321 IC₅₀ values were determined with microbroth dilution assays in Nunc 96-well plates. Vehicle
322 controls consisted of 1:75 dilutions of DMSO in 10:90 inoculated with PA14 or its mutants as described
323 in Growth Curves. Sterile controls consisted of 1:75 dilutions of DMSO in 10:90. Seven serially diluted
324 concentrations of TS – with 17 µg/mL being the highest final concentration – was set up in triplicate.
325 Tests were done with 1:75 dilutions of each TS concentration in 10:90 inoculated with PA14 or its
326 mutants as described in Growth Curves. Plates were sealed to prevent evaporation and incubated with
327 shaking at 200 rpm, 16h, 37°C. The OD₆₀₀ of the plates was read (Multiskan Go - Thermo Fisher
328 Scientific) and used to calculate IC₅₀. The final volume of each well was 150 µL and each experiment was
329 repeated at least three times.

330 Checkerboard assays were set-up using Nunc 96-well plates in an 8-well by 8-well format. Two
331 columns were allocated for vehicle controls and two columns for sterility controls. Vehicle controls
332 contained 2 µL DMSO + 2 µL DFP solvent for checkerboards with TS and DFP or 4 µL DMSO for TS and
333 DSX, in 146 µL of 10:90 inoculated with PA14 or PAO1-KP as described in Growth Curves. Sterile controls
334 contained the same components in 10:90, without cells. Serial dilutions of TS – with 17 µg/mL being the
335 highest final concentration – was added along the ordinate of the checkerboard (increasing
336 concentration from bottom to top) whereas serial dilutions of DFP or DSX – with 512 µg/mL being the
337 highest final concentration – was added along the abscissa (increasing concentration from left to right).
338 The final volume of each well was 150 µL and each checkerboard was repeated at least three times.
339 Plates were incubated and the final OD₆₀₀ determined as detailed above.

340 **Clinical isolates testing**

341 Clinical isolates of *P. aeruginosa* and *A. baumannii* were inoculated from -80°C stocks into 200 µL LB
342 broth and grown with shaking at 200 rpm, 16h, 37°C. in Nunc 96-well plates. The overnight cultures
343 were subcultured (1:25 dilution) into 10:90 and grown with shaking at 200 rpm, 2h, 37°C. Vehicle
344 controls consisted of 4 µL of DMSO, 144µL 10:90 and 2 µL of subculture. Sterile controls consisted of 4
345 µL of DMSO and 146µL 10:90. Test samples consisted of 2 µL of TS (final concentration of 5 µM, 8.3

346 $\mu\text{g/ml}$), 2 μL of DMSO (or DSX, final concentration of 86 μM , 32 $\mu\text{g/mL}$), 144 μL 10:90 and 2 μL of
347 subculture. The final volume of each well was 150 μL and each checkerboard was repeated at least three
348 times. Plates were incubated with shaking at 200 rpm, 16h, 37°C and OD₆₀₀ was measured (Multiskan Go
349 - Thermo Fisher Scientific). The results were plotted as percent of control (wells containing only DMSO)
350 using Prism (GraphPad).

351 REFERENCES

- 352 1. Zabawa TP, Pucci MJ, Parr TR, Jr., Lister T. 2016. Treatment of Gram-negative bacterial infections
353 by potentiation of antibiotics. *Curr Opin Microbiol* 33:7-12.
- 354 2. Blair JM, Webber MA, Baylay AJ, Ogbolu DO, Piddock LJ. 2015. Molecular mechanisms of
355 antibiotic resistance. *Nat Rev Microbiol* 13:42-51.
- 356 3. Hall CW, Mah TF. 2017. Molecular mechanisms of biofilm-based antibiotic resistance and
357 tolerance in pathogenic bacteria. *FEMS Microbiol Rev* 41:276-301.
- 358 4. Kalan L, Wright GD. 2011. Antibiotic adjuvants: multicomponent anti-infective strategies. *Expert*
359 *Rev Mol Med* 13:e5.
- 360 5. Tacconelli E, Carrara E, Savoldi A, Harbarth S, Mendelson M, Monnet DL, Pulcini C, Kahlmeter G,
361 Kluytmans J, Carmeli Y, Ouellette M, Outterson K, Patel J, Cavalieri M, Cox EM, Houchens CR,
362 Grayson ML, Hansen P, Singh N, Theuretzbacher U, Magrini N, Group WHOPPLW. 2018.
363 Discovery, research, and development of new antibiotics: the WHO priority list of antibiotic-
364 resistant bacteria and tuberculosis. *Lancet Infect Dis* 18:318-327.
- 365 6. Fothergill JL, Winstanley C, James CE. 2012. Novel therapeutic strategies to counter
366 *Pseudomonas aeruginosa* infections. *Expert Rev Anti Infect Ther* 10:219-35.
- 367 7. Rybtke M, Hultqvist LD, Givskov M, Tolker-Nielsen T. 2015. *Pseudomonas aeruginosa* Biofilm
368 Infections: Community Structure, Antimicrobial Tolerance and Immune Response. *J Mol Biol*
369 427:3628-45.
- 370 8. Burrows LL. 2018. The Therapeutic Pipeline for *Pseudomonas aeruginosa* Infections. *ACS Infect*
371 *Dis* 4:1041-1047.
- 372 9. Nguyen L, Garcia J, Gruenberg K, MacDougall C. 2018. Multidrug-Resistant *Pseudomonas*
373 Infections: Hard to Treat, But Hope on the Horizon? *Curr Infect Dis Rep* 20:23.
- 374 10. Page MG, Heim J. 2009. Prospects for the next anti-*Pseudomonas* drug. *Curr Opin Pharmacol*
375 9:558-65.

- 376 11. Wenderska IB, Chong M, McNulty J, Wright GD, Burrows LL. 2011. Palmitoyl-DL-carnitine is a
377 multitarget inhibitor of *Pseudomonas aeruginosa* biofilm development. *Chembiochem* 12:2759-
378 66.
- 379 12. Ejim L, Farha MA, Falconer SB, Wildenhain J, Coombes BK, Tyers M, Brown ED, Wright GD. 2011.
380 Combinations of antibiotics and nonantibiotic drugs enhance antimicrobial efficacy. *Nat Chem*
381 *Biol* 7:348-50.
- 382 13. Hoffman LR, D'Argenio DA, MacCoss MJ, Zhang Z, Jones RA, Miller SI. 2005. Aminoglycoside
383 antibiotics induce bacterial biofilm formation. *Nature* 436:1171-5.
- 384 14. Linares JF, Gustafsson I, Baquero F, Martinez JL. 2006. Antibiotics as intermicrobial signaling
385 agents instead of weapons. *Proc Natl Acad Sci U S A* 103:19484-9.
- 386 15. Jones C, Allsopp L, Horlick J, Kulasekara H, Filloux A. 2013. Subinhibitory concentration of
387 kanamycin induces the *Pseudomonas aeruginosa* type VI secretion system. *PLoS One* 8:e81132.
- 388 16. Oliveira NM, Martinez-Garcia E, Xavier J, Durham WM, Kolter R, Kim W, Foster KR. 2015. Biofilm
389 Formation As a Response to Ecological Competition. *PLoS Biol* 13:e1002191.
- 390 17. Ahmed MN, Porse A, Sommer MOA, Hoiby N, Ciofu O. 2018. Evolution of Antibiotic Resistance in
391 Biofilm and Planktonic *Pseudomonas aeruginosa* Populations Exposed to Subinhibitory Levels of
392 Ciprofloxacin. *Antimicrob Agents Chemother* 62.
- 393 18. Ranieri MR, Whitchurch CB, Burrows LL. 2018. Mechanisms of biofilm stimulation by
394 subinhibitory concentrations of antimicrobials. *Curr Opin Microbiol* 45:164-169.
- 395 19. Delcour AH. 2009. Outer membrane permeability and antibiotic resistance. *Biochim Biophys*
396 *Acta* 1794:808-16.
- 397 20. Cox G, Wright GD. 2013. Intrinsic antibiotic resistance: mechanisms, origins, challenges and
398 solutions. *Int J Med Microbiol* 303:287-92.
- 399 21. Zlitni S, Ferruccio LF, Brown ED. 2013. Metabolic suppression identifies new antibacterial
400 inhibitors under nutrient limitation. *Nat Chem Biol* 9:796-804.
- 401 22. Weisblum B, Demohn V. 1970. Thiostrepton, an inhibitor of 50S ribosome subunit function. *J*
402 *Bacteriol* 101:1073-5.
- 403 23. Gartel AL. 2008. FoxM1 inhibitors as potential anticancer drugs. *Expert Opin Ther Targets*
404 12:663-5.
- 405 24. Aminake MN, Schoof S, Sologub L, Leubner M, Kirschner M, Arndt HD, Pradel G. 2011.
406 Thiostrepton and derivatives exhibit antimalarial and gametocytocidal activity by dually
407 targeting parasite proteasome and apicoplast. *Antimicrob Agents Chemother* 55:1338-48.

- 408 25. Bibb MJ, Bibb MJ, Ward JM, Cohen SN. 1985. Nucleotide sequences encoding and promoting
409 expression of three antibiotic resistance genes indigenous to *Streptomyces*. *Mol Gen Genet*
410 199:26-36.
- 411 26. Dunstan MS, Hang PC, Zelinskaya NV, Honek JF, Conn GL. 2009. Structure of the thiostrepton
412 resistance methyltransferase-S-adenosyl-L-methionine complex and its interaction with
413 ribosomal RNA. *J Biol Chem* 284:17013-20.
- 414 27. Sezonov G, Joseleau-Petit D, D'Ari R. 2007. *Escherichia coli* physiology in Luria-Bertani broth. *J*
415 *Bacteriol* 189:8746-9.
- 416 28. Vogel HJ, Bonner DM. 1956. Acetylornithinase of *Escherichia coli*: partial purification and some
417 properties. *J Biol Chem* 218:97-106.
- 418 29. Pletzer D, Braun Y, Dubiley S, Lafon C, Kohler T, Page MGP, Mourez M, Severinov K, Weingart H.
419 2015. The *Pseudomonas aeruginosa* PA14 ABC Transporter NppA1A2BCD Is Required for Uptake
420 of Peptidyl Nucleoside Antibiotics. *J Bacteriol* 197:2217-2228.
- 421 30. Pletzer D, Braun Y, Weingart H. 2016. Swarming motility is modulated by expression of the
422 putative xenosiderophore transporter SppR-SppABCD in *Pseudomonas aeruginosa* PA14.
423 *Antonie Van Leeuwenhoek* 109:737-53.
- 424 31. Grinter R, Milner J, Walker D. 2013. Beware of proteins bearing gifts: protein antibiotics that use
425 iron as a Trojan horse. *FEMS Microbiol Lett* 338:1-9.
- 426 32. Braun V, Pramanik A, Gwinner T, Koberle M, Bohn E. 2009. Sideromycins: tools and antibiotics.
427 *Biometals* 22:3-13.
- 428 33. Denayer S, Matthijs S, Cornelis P. 2007. Pyocin S2 (Sa) kills *Pseudomonas aeruginosa* strains via
429 the FpvA type I ferripyoverdine receptor. *J Bacteriol* 189:7663-8.
- 430 34. Elfarash A, Wei Q, Cornelis P. 2012. The soluble pyocins S2 and S4 from *Pseudomonas*
431 *aeruginosa* bind to the same FpvAI receptor. *Microbiologyopen* 1:268-75.
- 432 35. Poole K, Neshat S, Heinrichs D. 1991. Pyoverdine-mediated iron transport in *Pseudomonas*
433 *aeruginosa*: involvement of a high-molecular-mass outer membrane protein. *FEMS Microbiol*
434 *Lett* 62:1-5.
- 435 36. Kwiatkowski JL. 2016. Current recommendations for chelation for transfusion-dependent
436 thalassemia. *Ann N Y Acad Sci* 1368:107-14.
- 437 37. Liberati NT, Urbach JM, Miyata S, Lee DG, Drenkard E, Wu G, Villanueva J, Wei T, Ausubel FM.
438 2006. An ordered, nonredundant library of *Pseudomonas aeruginosa* strain PA14 transposon
439 insertion mutants. *Proc Natl Acad Sci U S A* 103:2833-8.

- 440 38. Harding CM, Hennon SW, Feldman MF. 2018. Uncovering the mechanisms of *Acinetobacter*
441 *baumannii* virulence. *Nat Rev Microbiol* 16:91-102.
- 442 39. Singer ME, Finnerty WR. 1988. Construction of an *Escherichia coli*-*Rhodococcus* shuttle vector
443 and plasmid transformation in *Rhodococcus* spp. *J Bacteriol* 170:638-45.
- 444 40. Townsley L, Shank EA. 2017. Natural-Product Antibiotics: Cues for Modulating Bacterial Biofilm
445 Formation. *Trends Microbiol* 25:1016-1026.
- 446 41. Maier L, Pruteanu M, Kuhn M, Zeller G, Telzerow A, Anderson EE, Brochado AR, Fernandez KC,
447 Dose H, Mori H, Patil KR, Bork P, Typas A. 2018. Extensive impact of non-antibiotic drugs on
448 human gut bacteria. *Nature* 555:623-628.
- 449 42. Arnison PG, Bibb MJ, Bierbaum G, Bowers AA, Bugni TS, Bulaj G, Camarero JA, Campopiano DJ,
450 Challis GL, Clardy J, Cotter PD, Craik DJ, Dawson M, Dittmann E, Donadio S, Dorrestein PC, Entian
451 KD, Fischbach MA, Garavelli JS, Goransson U, Gruber CW, Haft DH, Hemscheidt TK, Hertweck C,
452 Hill C, Horswill AR, Jaspars M, Kelly WL, Klinman JP, Kuipers OP, Link AJ, Liu W, Marahiel MA,
453 Mitchell DA, Moll GN, Moore BS, Muller R, Nair SK, Nes IF, Norris GE, Olivera BM, Onaka H,
454 Patchett ML, Piel J, Reaney MJ, Rebuffat S, Ross RP, Sahl HG, Schmidt EW, Selsted ME, et al.
455 2013. Ribosomally synthesized and post-translationally modified peptide natural products:
456 overview and recommendations for a universal nomenclature. *Nat Prod Rep* 30:108-60.
- 457 43. Kelly WL, Pan L, Li C. 2009. Thiostrepton biosynthesis: prototype for a new family of
458 bacteriocins. *J Am Chem Soc* 131:4327-34.
- 459 44. Baumann S, Schoof S, Bolten M, Haering C, Takagi M, Shin-ya K, Arndt HD. 2010. Molecular
460 determinants of microbial resistance to thiopeptide antibiotics. *J Am Chem Soc* 132:6973-81.
- 461 45. Asensio C, Perez-Diaz JC. 1976. A new family of low molecular weight antibiotics from
462 enterobacteria. *Biochem Biophys Res Commun* 69:7-14.
- 463 46. Mathavan I, Zirah S, Mehmood S, Choudhury HG, Goulard C, Li Y, Robinson CV, Rebuffat S, Beis
464 K. 2014. Structural basis for hijacking siderophore receptors by antimicrobial lasso peptides. *Nat*
465 *Chem Biol* 10:340-2.
- 466 47. Anderson B, Hodgkin DC, Viswamitra MA. 1970. The structure of thiostrepton. *Nature* 225:233-
467 5.
- 468 48. Jonker HR, Baumann S, Wolf A, Schoof S, Hiller F, Schulte KW, Kirschner KN, Schwalbe H, Arndt
469 HD. 2011. NMR structures of thiostrepton derivatives for characterization of the ribosomal
470 binding site. *Angew Chem Int Ed Engl* 50:3308-12.

- 471 49. White P, Joshi A, Rassam P, Housden NG, Kaminska R, Goult JD, Redfield C, McCaughey LC,
472 Walker D, Mohammed S, Kleanthous C. 2017. Exploitation of an iron transporter for bacterial
473 protein antibiotic import. *Proc Natl Acad Sci U S A* 114:12051-12056.
- 474 50. Zhang F, Kelly WL. 2012. In vivo production of thiopeptide variants. *Methods Enzymol* 516:3-24.
- 475 51. Nicolaou KC, Zak M, Rahimpour S, Estrada AA, Lee SH, O'Brate A, Giannakakou P, Ghadiri MR.
476 2005. Discovery of a biologically active thiostrepton fragment. *J Am Chem Soc* 127:15042-4.
- 477 52. Schaible UE, Kaufmann SH. 2004. Iron and microbial infection. *Nat Rev Microbiol* 2:946-53.
- 478 53. Nairz M, Schroll A, Sonnweber T, Weiss G. 2010. The struggle for iron - a metal at the host-
479 pathogen interface. *Cell Microbiol* 12:1691-702.
- 480 54. Cassat JE, Skaar EP. 2013. Iron in infection and immunity. *Cell Host Microbe* 13:509-519.
- 481 55. Bleich R, Watrous JD, Dorrestein PC, Bowers AA, Shank EA. 2015. Thiopeptide antibiotics
482 stimulate biofilm formation in *Bacillus subtilis*. *Proc Natl Acad Sci U S A* 112:3086-91.
- 483 56. Huang J, Shi J, Molle V, Sohlberg B, Weaver D, Bibb MJ, Karoonuthaisiri N, Lih CJ, Kao CM,
484 Buttner MJ, Cohen SN. 2005. Cross-regulation among disparate antibiotic biosynthetic pathways
485 of *Streptomyces coelicolor*. *Mol Microbiol* 58:1276-87.

486

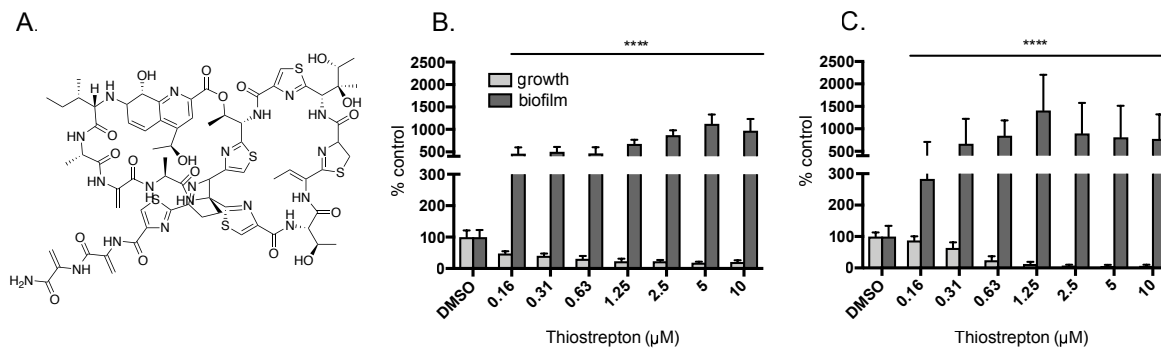
487

488 **Table 1.** Susceptibility of *P. aeruginosa* mutants to thiostrepton in VBMM.

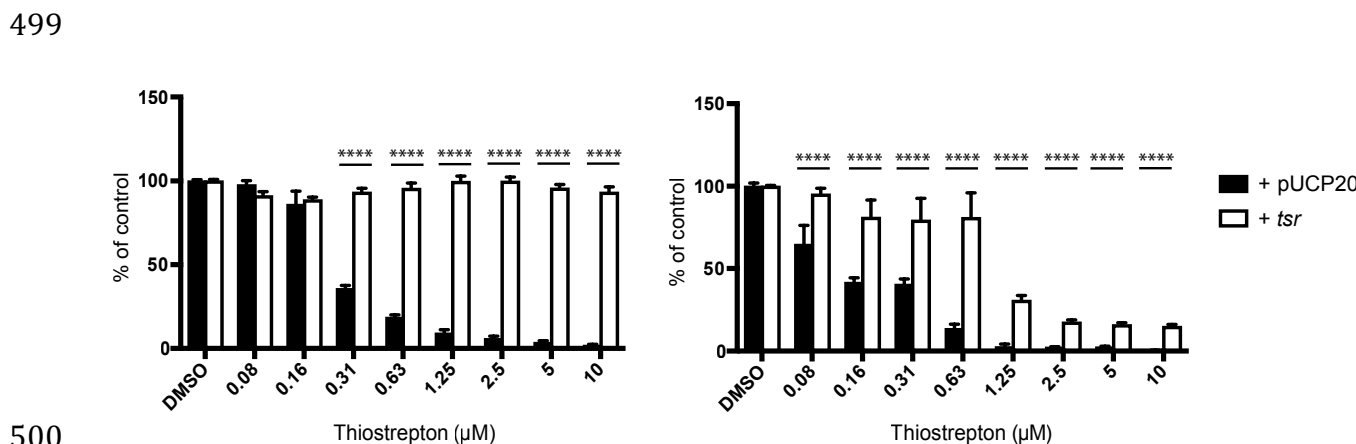
Strain	Gene	Function	IC ₅₀ µg/ml	IC ₅₀ µM
PA14	N/A	Wild type strain	0.26	0.16
<i>fpvA</i> ::Mar2xT7	PA2398	Type 1 ferripyoverdine receptor	3.68	2.21
<i>fpvB</i> ::Mar2xT7	PA4168	Alternate Type 1 ferripyoverdine receptor	1.83	1.10
<i>pvdA</i> ::Mar2xT7	PA2386	L-ornithine N5-oxygenase	0.26	0.16
Δ <i>fpvA</i> <i>fpvB</i> ::Mar2xT7	PA2398, PA4168	Type I ferripyoverdine receptor, Alternate type I ferripyoverdine receptor	6.93	4.16
Δ <i>fpvA</i> <i>fpvB</i> ::Mar2xT7 + pUCP20	PA2398, PA4168	Type I ferripyoverdine receptor, Alternate type I ferripyoverdine receptor	4.20	2.52
Δ <i>fpvA</i> <i>fpvB</i> ::Mar2xT7 + pUCP20- <i>fpvB</i>	PA2398, PA4168	Type I ferripyoverdine receptor, Alternate type I ferripyoverdine receptor	2.80	1.68
<i>fptA</i> ::Mar2xT7	PA4221	Pyochelin receptor	0.26	0.16
PA1322::Mar2xT7	PA1322	Probable TonB-dependent receptor	0.26	0.16
PA4837::Mar2xT7	PA4837	Probable outer membrane protein precursor	0.26	0.16
<i>foxA</i> ::Mar2xT7	PA2466	Ferrioxamine receptor FoxA	0.26	0.16
<i>fiuA</i> ::Mar2xT7	PA0470	Ferrichrome receptor FiuA	0.26	0.16
<i>pirA</i> ::Mar2xT7	PA0931	Alternate enterobactin receptor	0.35	0.21
<i>pfeA</i> ::Mar2xT7	PA2688	Enterobactin receptor	0.26	0.16
<i>hasR</i> ::Mar2xT7	PA3408	Heme uptake outer membrane receptor	0.35	0.21
<i>fvbA</i> ::Mar2xT7	PA4516	Vibriobactin receptor	0.26	0.16
<i>piuA</i> ::Mar2xT7	PA4514	Hydroxamate-type ferrisiderophore receptor	0.35	0.21
PA0151::Mar2xT7	PA0151	Probable TonB-dependent receptor	0.26	0.16

chtA::Mar2xT7	PA4675	Aerobactin, Rhizobactin 1021, Schizokinen receptor	0.59	0.36
phuR::Mar2xT7	PA4710	Heme/Hemoglobin uptake receptor precursor	0.26	0.16

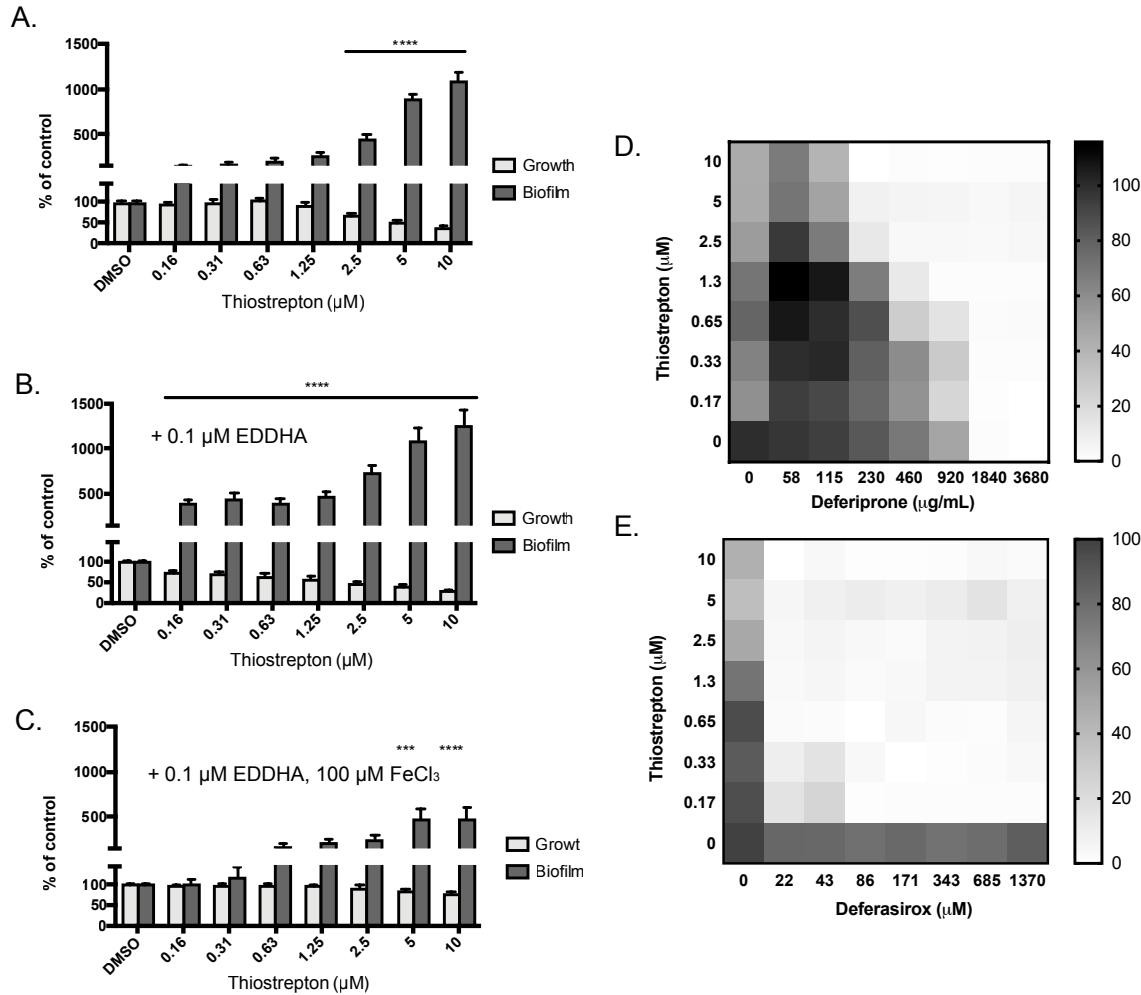
489



490
 491 **Figure 1. Thiostrepton stimulates *P. aeruginosa* biofilm formation.** **A.** Structure of thiostrepton (TS). **B.**
 492 TS stimulated biofilm formation (absorbance of eluted crystal violet at 600 nm, plotted as percent of the
 493 DMSO control) of *P. aeruginosa* PAO1 and decreased planktonic cell density (optical density at 600 nm,
 494 plotted as percent of the DMSO control) in 10:90 medium in a dose-dependent manner, up to its
 495 maximum soluble concentration of 10 μM (17 μg/ml). **C.** In VBMM, PAO1 biofilm formation was
 496 stimulated by TS, while planktonic cell density decreased below the level of detection at concentrations
 497 above 1.25 μM. Y-axes are split to better display growth values. Assays were performed at least 3 times
 498 in triplicate. **** p < 0.0001



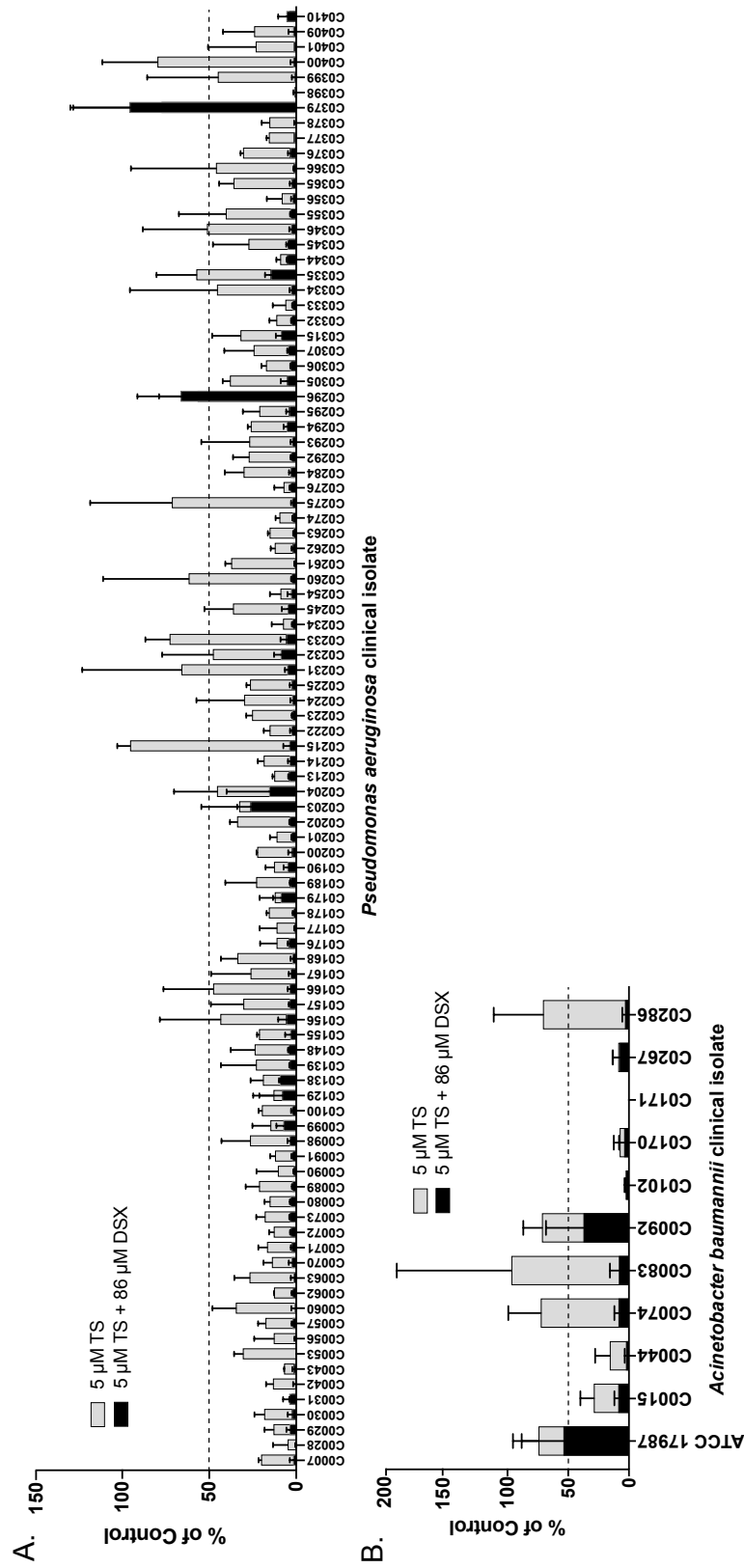
500
 501 **Figure 2. Expression of Tsr in trans reduces susceptibility of *P. aeruginosa* to thiostrepton.** Expression
 502 of the *tsr* gene from *Streptomyces azureus* in trans from pUCP20 in two strains of *P. aeruginosa* reduced
 503 their susceptibility to TS in VBMM, suggesting it inhibits growth via its canonical mode of action,
 504 disrupting translation. **A.** Growth of PAO1 (OD₆₀₀ plotted as percent of the DMSO control); **B.** Growth of
 505 PA14. Each assay was performed at least 3 times in triplicate. **** p < 0.0001



506

507 **Figure 3. Thiostrepton activity is potentiated by iron chelators.** Biofilm stimulation by TS in 10:90
 508 medium increased in the presence of 0.1 μM EDDHA, a cell-impermeant iron chelator, while further
 509 addition of 100 μM FeCl_3 increased the concentration of TS required for biofilm stimulation and growth
 510 inhibition. **A.** PAO1 growth (OD_{600}) and biofilm (absorbance of CV at 600 nm) in 10:90 medium alone; **B.**
 511 10:90 plus 0.1 μM EDDHA; **C.** 10:90 plus 0.1 μM EDDHA and 100 μM FeCl_3 . Checkerboard assays plotted
 512 as percent growth of the DMSO control (0,0 μM at lower left) showed that TS activity against PAO1 was
 513 potentiated by FDA-approved iron chelators, **D.** deferiprone and **E.** deferasirox. The highest
 514 concentrations of DFP (3680 μM) and DSX (1370 μM) are each equal to 512 $\mu\text{g/ml}$. Each assay was
 515 performed at least 3 times. *** $p < 0.001$; **** $p < 0.0001$

516



518 **Figure 4. Thiostrepton inhibits growth of multidrug-resistant clinical isolates.** The growth of most
519 clinical isolates of **A. *P. aeruginosa*** and **B. *Acinetobacter baumannii*** resistant to multiple antibiotics (see
520 **Supplementary Table S2** for antibiograms) was inhibited by 5 μ M (8.3 μ g/ml) TS in 10:90 medium (grey
521 bars). TS activity was potentiated by the addition of 86 μ M deferasirox (DSX; 32 μ g/ml; black bars). Each
522 assay was performed at least 3 times and the results plotted as percent of the DMSO-only growth
523 control (OD_{600}) using Prism (GraphPad). Error bars equal one standard deviation.